1

Introduction to Desalination

Jesa Singh, Vinayagam Sivabalan, and Bhajan Lal

1.1 Coping with Water Scarcity

Climate change and population growth have significantly altered global water resources in the twentieth century and are likely to pose more challenges in the future. One of the greatest of these challenges is freshwater security and equitability. Freshwater is used primarily for sustenance and in various industries that enable today's high living standards, such as mining, agriculture, and power generation. As evident in Figure 1.1, irrigation consumes the most water among the industrial uses [1]. In the agricultural sector, maintaining an adequate water supply is of foremost importance in ensuring optimal conditions for managing livestock and raising crops, both of which are vital to the wellness of the general population and economies. Lack of freshwater can also affect material and energy-related industries by ultimately decreasing product quality.

Groundwater is an essential source of freshwater, meeting the domestic needs of about half of the global population and more than a third of global consumptive irrigation demand. In the United States (US), groundwater resources provide over fifty billion gallons per day for agricultural needs and drinking water to about half the total population. Nearly all of the US rural population depends on groundwater resources. In areas where surface water such as lakes and rivers are scarce or inaccessible, groundwater also supplies much of the habitant's hydrologic needs.

Groundwater depletion, defined as long-term water-level declines caused by sustained groundwater pumping, is a key issue associated with groundwater use. Groundwater depletion is significant in most irrigated regions of the world where millions of people reside [2]. Many areas of the United States are experiencing groundwater depletion, which can result in water table lowering,

Gas Hydrate in Water Treatment: Technological, Economic, and Industrial Aspects,
First Edition. Bhajan Lal and Sirisha Nallakukkala.

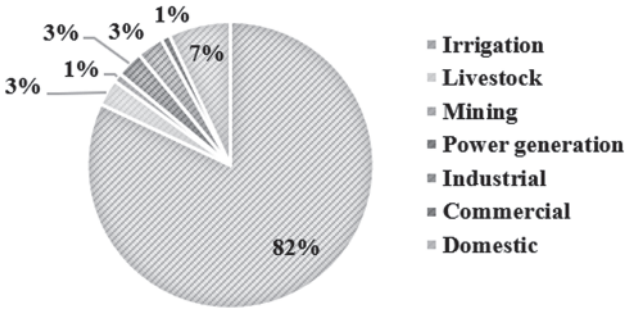

Figure 1.1 Freshwater consumption.

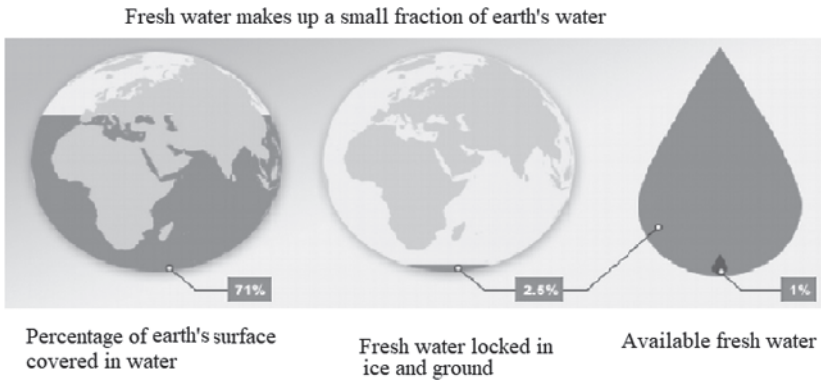

Figure 1.2 Earth's freshwater resources.

leading to the reduction of freshwater in streams and lakes [2]. While the expansion of groundwater-based irrigation has helped to meet increased food demands, it has resulted in several environmental implications. Groundwater depletion has now become one of the most prominent challenges for food and water security.

Figure 1.2 shows the natural sources of water that make up 71% of our planet [3]. However, out of this 71%, a mere 2.5% is freshwater. From this 2.5%, we only have easy access to approximately 1%, while the remaining 1.5% are trapped in glaciers, ice caps, and deep underground, making it economically unfeasible to access efficiently [4]. The accessibility of freshwater poses a clear problem, as the finite supply may not be enough to upkeep the ever increasing human population.

Water scarcity is a situation where there is not enough water to meet essential needs, like drinking or growing food. Total water consumption has been increasing at a rate of more than twice the rate of population increase in the last century. By 2025, approximately 1.8 billion people will be living in arid regions with absolute water scarcity, while two-thirds of the remaining population will be living under the looming shadow of water scarcity [5]. Figure 1.3 shows the trend in water scarcity around the globe [6].

In the event of water scarcity, the most typical symptom is the rise of price in freshwater, due to its inability to meet the required demands and expectations. Compounded with the population growth, it will eventually arrive at a point where there simply is not enough to go around. The general populace tends to not recognize the limits of water supplies, and would rather focus on acquiring additional supplies rather than managing existing supplies. This is repeated in many basins around the world. Because we overbuild and expect too much, we arrive at a situation where there is not enough water to go around. Moreover, when water is reallocated, it tends to meet the needs of the wealthier rather than the poor or marginalized. Cases of successful water management that have effectively tackled water scarcity exist and must be critically examined to prevent the devastating effects of abject resource mismanagement [7].

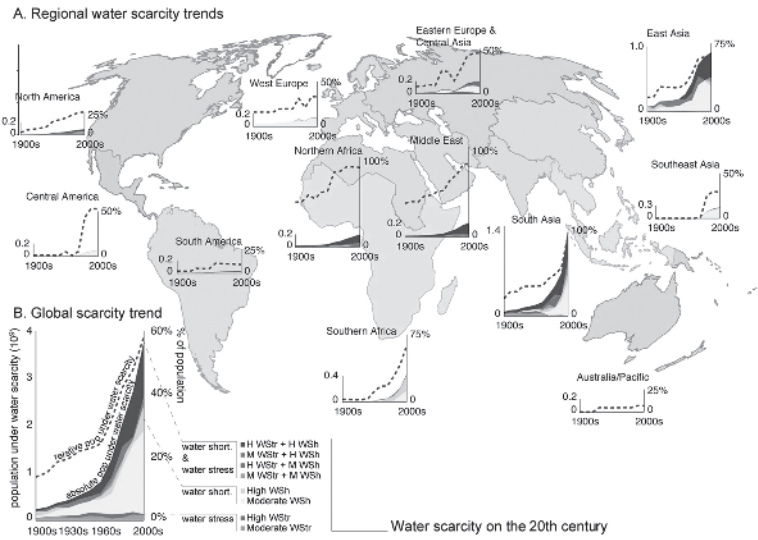

Figure 1.3 Water scarcity trajectories. Filled graphs represent the absolute population under water scarcity (in billions) while dashed lines represent the population relative to the total regional population [6].

A process called desalination can mitigate freshwater scarcity by converting seawater, which is unsuitable for either human consumption or industrial and agricultural operations, into freshwater. Various desalination methods have been developed over the last several decades to augment freshwater supplies in arid regions [4] including, multistage flash distillation (MSF), multi-effect distillation (MED), reverse osmosis (RO), solar evaporation, and freeze and thaw (cryodesalination). These processes are thoroughly discussed in Chapter 2.

Currently, most desalination plants worldwide are RO plants, while some use MSF. Together, these two processes account for 90% of the global desalination capacity. Generally, the seawater desalination process separates seawater into two streams. One stream is freshwater, while concentrated brine makes up the other. Achieving this separation requires a certain amount of energy and equipment specific to the process. Commercially, the two most important processes are MSF and RO, with MSF being the more dominant of the two in the twentieth century. In 1998, MSF plants accounted for 78% of the global desalination capacity, while RO only accounted for 10%. With time and advancements in technology, RO has grown in importance as a desalination process due to its lower cost and simplicity [4]. Conventional desalination methods may seem to be the answer everyone is looking for to solve water scarcity. However, that could not be further from the truth as conventional desalination methods incur high costs in terms of operation and maintenance [9]. Due to this, many arid regions in the world are unable to afford these technologies as an augmented freshwater source, hardly solving their water insecurity issue. Continuous research is being done in the desalination fields, with gas hydrate formation technology as one of the latest desalination technologies currently in testing. Although gas hydrate-based desalination technology began development way back in 1940, details regarding the technology are very scarce, though it shows promising potential. The contents of this book aim to highlight the growing developments in gas hydrate-based desalination.

1.2 Origin of Gas Hydrates

Gas hydrates are nonstoichiometric crystalline complexes containing water and guest molecules that form under low temperature (T) and high pressure (P) conditions. Guest molecules, such as methane (CH_4), propane (C_3H_8), and carbon dioxide (CO_2), are bundled in cages formed by hydrogen-bound water molecules. These cages are stabilized by van der Waals forces between guest molecules and water molecules. Gas hydrates are at the center of research within sustainable chemistry because of their innovative applications in a wide

range of scientific and industrial contexts, such as gas exploration and production, energy storage, and CO_2 sequestration.

Under favorable conditions of temperature and pressure (P–T), i.e. low T and high P values, the hydration reaction of the guest species, or hydrate former F, is given by Eq. (1.1):

$$F + xH_2O = F'' \, xH_2O, \tag{1.1}$$

where "x" is the hydration number [10].

So far, three key kinds of gas hydrate structures have been determined, namely s1, sII, and sH structures. The shape, type, and size of the guest molecule greatly impact the type of gas hydrate structure formed. The shape and size of the hydrate cavities in the cages govern the structure difference, while the type and size of gas molecules indicate the type of hydrate formed. A cubic meter of hydrate constitutes about 180 m^3 of gas. A unit cell of sI hydrate consists of six large ($5^{12}\,6^2$) cavities and two small (5^{12}) cavities made up of 46 H_2O molecules. Guest molecules with a diameter of less than 6 Å, such as CH_4, C_2H_6, CO_2, and hydrogen sulfide (H_2S), form the sI structure. An sII hydrate unit cell contains 16 small (5^{12}) and eight large cavities ($5^{12}6^4$) formed by 136 H_2O molecules and guest molecules such as C_3H_8, isobutane. Smaller molecules like nitrogen, whose diameter is less than 4.2 Å, are exceptions and form sII structure when used as pure hydrate formers. sH structure consists of three cavities that are basic 5^{12}, $4^3 5^6 6^3$, and $5^{12}6^8$ cages. Smaller molecules, such as CH_4, xenon (Xe), or H_2S, help to stabilize the structure by occupying the small cages. Molecules that are larger in size (7 Å < d < 9 Å), such as isopentane and neohexane, can form sH structures when accompanied by smaller molecules such as N_2, H_2S, and CH_4 [10].

1.3 Concept of Hydrate Formation

Hydrate formation is a physical process (crystallization) that includes nucleation, growth, and dissociation. The nucleation process starts once the essential requirements for the formation hydrate formation are accessible, i.e. high pressure, low temperature, a hydrate former, and the necessary amount of water. The stability of hydrate formation mostly relies on the pressure, temperature, type, composition, and thermodynamic behavior of the hydrate former. During the nucleation process, the water molecules group up on the sides of the hydrate former to form a whole or an incomplete embryo crystal. During this phase, certain variables like driving force, activation energy, the critical size of nuclei, and nucleation rate are critical. Based on pressure–temperature

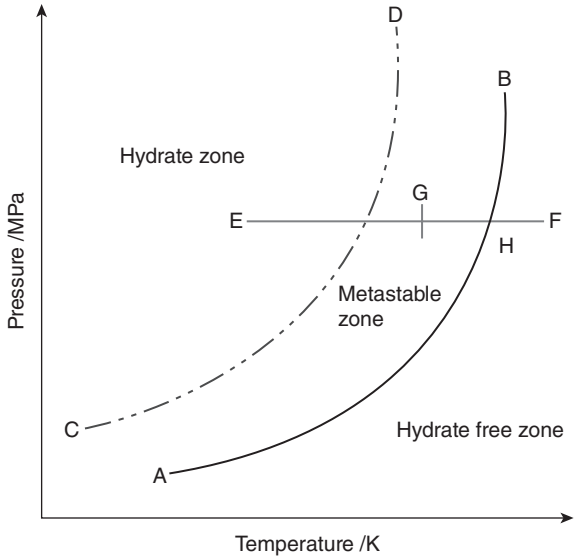

Figure 1.4 The formation of hydrate as a function of driving force (subcooling).

(P–T) plots, the formation of hydrate, nucleation, and the metastability of the hydrates can be estimated, as shown in Figure 1.4.

In Figure 1.4, the AB curve signifies the equilibrium curve and curve CD signifies supersaturation that demonstrates the limit of the metastability region. At position F, superheated state, there is no sign of the growth of the crystal. If nucleation starts at position H, then hydrates will start to form at position G. If the driving force (subcooling temperature) increases, then hydrate formation increases from position G toward E. Nucleation initiates rapidly and crystallizes left of the curve CD [10]. The cages tend to become unstable after nucleation completes and dissolve or grow into hydrates, thus forming metastable nuclei. Phase equilibrium data makes it possible to predict whether the hydrate former inhibits or promotes hydrate formation. The development of a hydrate depends on the interaction among the two fluids, temperature, pressure, mixing pattern, water history, and subcooling, as extensively discussed by [10, 11]. The knowledge of phase equilibrium conditions of various hydrate formers in wastewater samples can successfully guide the choice of experimental temperature and pressure. Several researchers have tried to identify the necessary parameters for hydrate-based water treatment by calculating the hydrate phase equilibria of refrigerants [12] and refrigerants in different salts like $MgCl_2$, NaCl, $CaCl_2$ [13, 14]. These

feasibility studies used a single solute at low concentrations, but there is a need to experimentally investigate the hydrate phase equilibria with mixed solutes at high concentrations.

1.4 Application of Gas Hydrate in Desalination

Gaseous hydrate-based promoters can be used to treat saline water, wastewater, and produced water. The pure water molecules, now in the solid form, can be recovered through the melting (dissociation) and separation process. During the formation of hydrate, impurities or metal ions are rejected into the residual water resulting in the formation of pure hydrate, which on melting results in pure water and gas. The rejected water is rich in metal ion content and can be reused in subsequent desalination runs. This approach has been investigated extensively in the past using CH_4 and CO_2 hydrates, but no industrial solutions presently exist for a variety of practical and economic issues. However, recent advances in clathrate promoter research have opened the way to more appropriate, resilient, and less expensive alternatives to CH_4 or CO_2 for desalination applications.

1.5 Phase Behavior and Thermodynamic Measurement

Hydrate phase equilibrium studies are generally performed at a constant volume approach. It includes filling the reactor vessel with a sufficient amount of water. The reactor is then submerged in the coolant bath consisting of ethylene glycol and water. Excess air present inside the reactor is purged with the hydrate former (CO_2) gas. Later, the reactor is further pressurized with CO_2 guest gas and stabilized at the desired experimental pressure conditions. Once the pressure of the system is stabilized, the temperature is reduced to the experimental temperature to enable hydrate formation. A sharp rise in temperature or reduction in pressure indicates that hydrate formation is occurring. As more gas is consumed, pressure continues to drop until the completion of hydrate formation. Subsequently, the temperature of the bath encompassing the reactor gradually increases, leading to the dissociation of the hydrates. As dissociation proceeds, the pressure inside the reactor increases due to the release of gas. When dissociation is complete, the reactor pressure restabilizes. These changes in the temperature and pressure throughout the experiment are recorded by the data acquisition system. Hydrate phase equilibrium of the

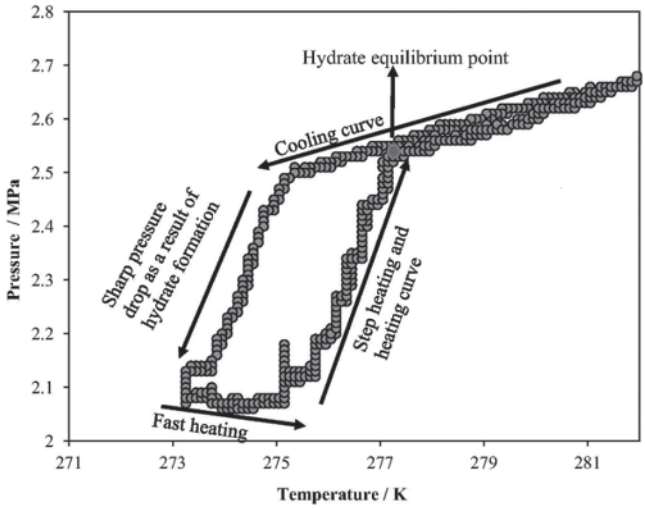

Figure 1.5 Pressure–temperature plot for CO_2 hydrate formation.

three phases (hydrate, liquid, and vapor) is achieved by sketching the intersection of (P–T) profiles of hydrate formation and dissociation mechanism, as shown in Figure 1.5 [15].

1.6 Kinetics of Hydrate Formation

A thorough understanding of the kinetics of hydrate is beneficial to (i) improve the formation of hydrates, such as storage of gas, separation of gas, and sequestration of gas [16, 17]; (ii) prevent hydrate development, particularly in the context of flow assurance [18]; and (iii) understand the rate of hydrate formation [19]. In comparison to gas hydrate dissociation [20], the investigation of hydrate formation is more confusing, as it involves nucleation followed by the growth phase.

The different steps of the hydrate nucleation process can be achieved as shown in Figure 1.6. Due to the gas solubility in liquid, the development of hydrates begins with an increase in gas intake. After the dissolution of gas into a liquid, the supersaturation phase begins when the operating temperature and pressure favor the formation of hydrates. There is a critical radius that must form during the induction time for nucleus stabilization; the hydrate nuclei must be larger than the critical radius. Any nuclei with a radius smaller than the critical radius would dissolve in the liquid phase. These critical radius

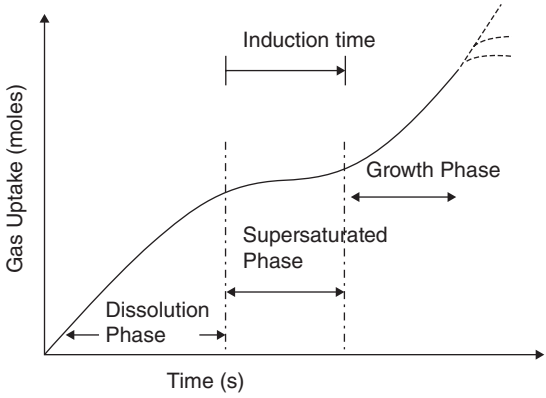

Figure 1.6 Phases in the hydrate formation process.

nuclei serve as the focal point for hydrate growth [21, 22], which is accompanied by a rise in gas intake.

Finally, depending on the mass transfer resistance, the gas intake may end at various phases, as illustrated in Figure 1.6 by the dotted lines. It is possible to break the mass transfer constraint at the gas–liquid interface using a stirrer or mixing mechanism. Hence, a further additional critical factor to be considered is the heat transfer mechanism to form hydrates faster. For faster hydrate formation phenomena to happen, the water surface area, gas dissolution rate, and contact must be enhanced. Hydrate formation is an exothermic reaction, so the heat generated during cooling should be eliminated in a batch or continuous approach to optimize the hydrate formation rate. The kinetics estimation variables are primarily utilized to comprehend and measure the formation kinetics following experiments. These variables are induction time, water to hydrate conversion, rate of hydrate formation, moles of gas consumed, and water recovery.

Generally, the evaluation of kinetic measurements is measured in a constant cooling batch approach. In the high-pressure reactor, a sufficient quantity of water is added. After that, the cell is transferred to the water bath containing water and ethylene glycol as coolant. Then the reactor is pressurized with the hydrate forming gas (CO_2) to the desired experimental pressure, and the temperature of the bath is set to the initial experimental condition. The system is left to stabilize before starting the experiment. After that, the system temperature is reduced to the desired experimental temperature by cooling. As cooling continues, the pressure reduces due to the hydrate formation. Simultaneously, due to the exothermic nature of hydrate formation, the temperature also increases.

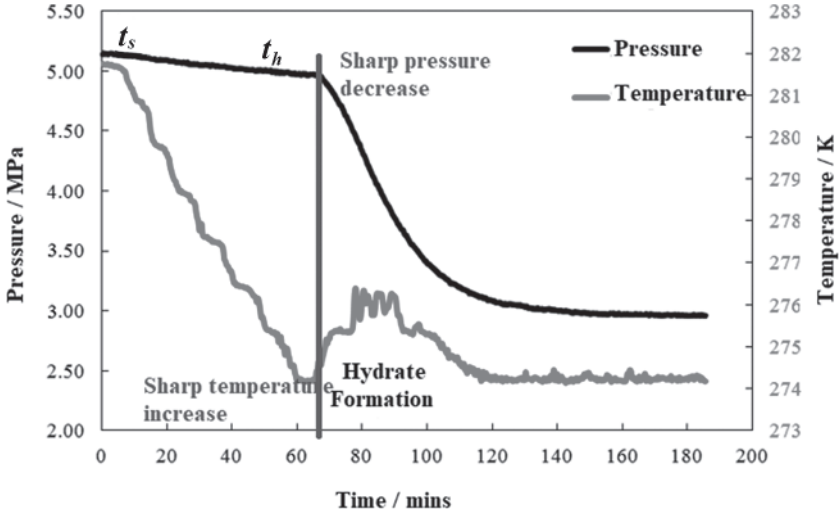

Figure 1.7 Temperature–pressure vs. time for CO_2 hydrate formation.

These changes in pressure and temperature are recorded by the data acquisition system. Once the hydrate formation is complete, the temperature and pressure become stable, as shown in Figure 1.7. Some of the kinetic parameters evaluated in terms of hydrate-based desalination are induction time, moles of gas used up, rate of hydrate formation, and water to hydrate conversion (mol%).

1.6.1 Induction Time

The time between the commencement of hydrate formation and the initial nucleation is known as the induction time. It is characterized by a rapid rise in temperature due to the exothermic nature of hydrate formation and a concomitant decrease in pressure owing to hydrate formation. It is written as presented in Eq. (1.2):

$$I_t = t_h - t_s, \tag{1.2}$$

where t_s is the system pressure and temperature to stabilize the initial experimental operating conditions, and t_h denotes the time taken for the noticeable hydrate to form [10].

1.6.2 Moles of Gas Used Up

The moles of gas used up is a critical variable that aids in determining the kinetics of the entire process. It reflects the quantity of gas spent throughout

the method, which is equivalent to the quantity of CO_2 gas that could potentially be stored in hydrates. It can be estimated from the experimental pressure and temperature using the real gas equation, where Δn_H is the difference between moles of gas consumed at time t and 0, as presented in Eq. (1.3):

$$\Delta n_H = \left[\frac{PV}{zRT}\right]0 - \left[\frac{PV}{zRT}\right]t, \tag{1.3}$$

where z, R, T, V and P are Pitzers correlation, the gas constant, temperature, gas phase volume and pressure, respectively.

1.6.3 Rate of Hydrate Formation

The forward difference approach is used to calculate the starting rate of hydrate formation, as given by Eq. (1.4) [22].

$$\left(\frac{d\Delta n_{H,\downarrow}}{dt}\right)\mathrm{t} = \frac{\left(\Delta n_{H,\downarrow}\right)\mathrm{t} + \Delta\mathrm{t} - \left(\Delta n_{H,\downarrow}\right)\mathrm{t}}{\Delta t} \tag{1.4}$$

1.6.4 Water to Hydrate Conversion

The proportion of water converted into hydrate (C_{wh}) is a key factor in hydrate formation kinetics and is influenced by salt. Equation (1.5) is used to determine C_{wh}:

$$C_{wh}(\%) = \frac{\Delta n_H * h^n}{n_{H_2O}} * 100, \tag{1.5}$$

where Δn_H is the moles of gas used for the hydrate formation process as calculated in Eq.(1.3), n_{H_2O} refers to the moles of water existing in the reactor, and h^{n} is the hydration number described as the number of water molecules essential to clathrate a single hydrate former molecule [23].

Water recovery signifies the volumetric process efficiency of the hydrate-based desalination process and can be estimated by Eq. (1.6), as given in the literature [24].

$$\text{Percentage water recovery} = \frac{\left(Volume\,of\,water\,converted\,to\,hydrate\right) * (F_h)}{Volume\,of\;feed\,solution} * 100 \tag{1.6}$$

Rejection of salt signifies the efficiency of the process in eliminating contaminants. The salt rejection or removal efficiency is estimated by Eq. (1.7) [24, 25].

$$\text{Percentage removal efficiency} = \frac{C_{A0} - C_A}{C_{A0}} * 100 \tag{1.7}$$

Here, C_{A0} is the initial concentration of effluent, and C_A is that in the dissociated water. From the ion concentration present in the feed sample and the generated water following hydrate dissociation, the rejection percentage of each ion might be computed. The system's performance improves as the rejection rate rises. The yield of water is estimated as:

$$\text{Water yield} = \frac{V_1}{V_0} * 100, \tag{1.8}$$

where V_0 is the initial volume of effluent, and V_1 is the volume of dissociated water.

1.7 Hydrate Decomposition

The dissociation of the hydrate is an important phase in hydrate-based desalination (HBD). Hydrate dissociation might be accomplished by three methods: (i) by depressurization [26], (ii) through thermal heating [27], and (iii) by chemical injection [28]. Depressurization involves lowering the pressure at the interface so that the equilibrium temperature of the hydrate is lower than the ambient temperature. The heat input is caused by the temperature gradient from the surroundings, and the hydrate dissociates as a result. Modeling the hydrate dissociation phenomena by depressurization is a current study focus among researchers. In thermal treatment, the pressure is kept constant by applying heat to dissociate the hydrate crystal. This is the preferred practice in research laboratories. Chemical injection involves injecting chemicals into the hydrate to dissociate it, which is risky owing to geomechanics instability and natural calamities. The hydrate dissociation necessitates the use of heat energy in order to melt the hydrate crystals by releasing water and gas.

The stability of the hydrate's formation is estimated by studying the hydrate decomposition. At the onset of the dissociation process, residual water is drained, and the freshwater is collected and analyzed post-dissociation. To begin the dissociation process, the reactor vessel is depressurized to about 10% over the hydrate equilibrium pressure after the formation of hydrates. Next, the temperature is permitted to stabilize by slowly increasing the bath temperature. As temperature increases, it passes through the hydrate equilibrium boundary conditions, and the hydrates begin to dissociate, thereby increasing the reactor pressure. As the dissociate progresses, the pressure becomes constant, indicating the completion of dissociation of hydrate. The dissociated hydrate is collected as freshwater, and the rejected ion-rich water can be further treated through the gas hydrate process.

References

1 Aitken, C.K., McMahon, T.A., Wearing, A.J., and Finlayson, B.L. (1994). Residential water use: Predicting and reducing consumption 1. *Journal of Applied Social Psychology* 24 (2): 136–158.

2 Dangar, S., Asoka, A., and Mishra, V. (2021). Causes and implications of groundwater depletion in India: A review. *Journal of Hydrology*, 596: 126103. doi: 10.1016/j.jhydrol.2021.12610352659.

3 Water In The West. (2013). Water and energy nexus: A literature review.

4 Khawaji, A.D., Kutubkhanah, I.K., and Wie, J.M. (2008). Advances in seawater desalination technologies. *Desalination* 221 (1–3): 47–69.

5 Molden, D. (2019). Scarcity of water or scarcity of management? *International Journal of Water Resources Development* 36 (2–3): 258–268.

6 Kummu, M., Guillaume, J.H., De Moel, H., Eisner, S., Flörke, M., Porkka, M., et al. (2016). The world's road to water scarcity: Shortage and stress in the 20th century and pathways towards sustainability. *Scientific Reports* 6 (1): 1–16.

7 Zheng, J., Cheng, F., Li, Y., Lü, X., and Yang, M. (2019). Progress and trends in hydrate based desalination (HBD) technology: A review. *Chinese Journal of Chemical Engineering* 27 (9): 2037–2043.

8 Karagiannis, I.C. and Soldatos, P.G. (2008). Water desalination cost literature: Review and assessment. *Desalination* 223 (1–3): 448–456.

9 Sloan, E.D. and Koh, C.A. (2008). *Clathrate Hydrates of Natural Gases*, 3e. Boca Raton: CRC Press.

10 Lal, B. and Nashed, O. (2019). *Chemical Additives for Gas Hydrates*. Springer Nature.

11 Liang, D., Guo, K., Wang, R., and Fan, S. (2001). Hydrate equilibrium data of 1, 1, 1, 2-tetrafluoroethane (HFC-134a), 1, 1-dichloro-1-fluoroethane (HCFC-141b) and 1, 1-difluoroethane (HFC-152a). *Fluid Phase Equilibria* 187: 61–70.

12 Ngema, P.T., Naidoo, P., Mohammadi, A.H., Richon, D., and Ramjugernath, D. (2016). Thermodynamic stability conditions of clathrate hydrates for refrigerant (R134a or R410a or R507) with $MgCl_2$ aqueous solution. *Fluid Phase Equilibria* 413: 92–98.

13 Ngema, P.T., Petticrew, C., Naidoo, P., Mohammadi, A.H., and Ramjugernath, D. (2014). Experimental measurements and thermodynamic modeling of the dissociation conditions of clathrate hydrates for (refrigerant+ NaCl+ water) systems. *Journal of Chemical & Engineering Data* 59 (2): 466–475.

14 Bavoh, C.B., Partoon, B., Lal, B., Gonfa, G., Foo Khor, S., and Sharif, A.M. (2017). Inhibition effect of amino acids on carbon dioxide hydrate. *Chemical Engineering Science* 171: 331–339. doi: 10.1016/j.ces.2017.05.046.

15 Babu, P., Kumar, R., and Linga, P. (2013). Pre-combustion capture of carbon dioxide in a fixed bed reactor using the clathrate hydrate process. *Energy* 50: 364–373.

16 Dashti, H., Yew, L.Z., and Lou, X. (2015). Recent advances in gas hydrate-based CO_2 capture. *Journal of Natural Gas Science and Engineering* 23: 195–207.

17 Lederhos, J.P., Long, J.P., Sum, A., Christiansen, R.L., and Sloan, E.D., Jr. (1996). Effective kinetic inhibitors for natural gas hydrates. *Chemical Engineering Science* 51 (8): 1221–1229.

18 Babu, P., Linga, P., Kumar, R., and Englezos, P. (2015). A review of the hydrate based gas separation (HBGS) process for carbon dioxide pre-combustion capture. *Energy* 85: 261–279.

19 Yin, Z., Chong, Z.R., Tan, H.K., and Linga, P. (2016). Review of gas hydrate dissociation kinetic models for energy recovery. *Journal of Natural Gas Science and Engineering* 35: 1362–1387.

20 Maini, B.B. and Bishnoi, P.R. (1981). Experimental investigation of hydrate formation behaviour of a natural gas bubble in a simulated deep sea environment. *Chemical Engineering Science* 36 (1): 183–189.

21 Khurana, M., Yin, Z., and Linga, P. (2017). A review of clathrate hydrate nucleation. *ACS Sustainable Chemistry & Engineering* 5 (12): 11176–11203.

22 Linga, P., Daraboina, N., Ripmeester, J.A., and Englezos, P. (2012). Enhanced rate of gas hydrate formation in a fixed bed column filled with sand compared to a stirred vessel. *Chemical Engineering Science* 68: 617–623. doi: 10.1016/j.ces.2011.10.030.

23 Babu, P., Nambiar, A., He, T., Karimi, I.A., Lee, J.D., Englezos, P., and Linga, P. (2018). A review of clathrate hydrate based desalination to strengthen energy–water nexus. *ACS Sustainable Chemistry & Engineering* 6 (7): 8093–8107.

24 Nallakukkala, S. and Lal, B. (2021). Seawater and produced water treatment via gas hydrate. *Journal of Environmental Chemical Engineering* 9 (2). doi: 10.1016/j.jece.2021.1050539 (2).

25 Li, D. and Liang, D. (2012). Seawater desalination plant and seawater desalination method. Patent CN102351255A.

26 Wang, Y., Li, X.S., Li, G., Zhang, Y., Li, B., and Chen, Z.Y. (2013). Experimental investigation into methane hydrate production during three-dimensional thermal stimulation with five-spot well system. *Applied Energy* 110: 90–97.

27 Li, G., Li, X.S., Tang, L.G., and Zhang, Y. (2007). Experimental investigation of production behavior of methane hydrate under ethylene glycol injection in unconsolidated sediment. *Energy & Fuels* 21 (6): 3388–3393.

28 Yang, S.H.B., Babu, P., Chua, S.F.S., and Linga, P. (2016). Carbon dioxide hydrate kinetics in porous media with and without salts. *Applied Energy* 162: 1131–1140. doi: 10.1016/j.apenergy.2014.11.052.